Research Square

Preprints are preliminary reports that have not undergone peer review.
They should not be considered conclusive, used to inform clinical practice,
or referenced by the media as validated information.

CT and Radiographic Assessment of Thoracic Skeletal Morphology in the Persian Squirrel (Sciurus anomalus)

Ghasem Akbari

g.akbari@tabrizu.ac.ir

University of Tabriz

Atabak Shokrollahi

University of Tabriz

Research Article

Keywords: Persian squirrel, thoracic cavity, anticlinal vertebra, morphometry, computed tomography

Posted Date: November 24th, 2026

DOI: https://doi.org/10.21203/rs.3.rs-11585986/v1

License: This work is licensed under a Creative Commons Attribution 4.0 International License.
Read Full License

Additional Declarations: No competing interests reported.

Abstract

Background: The Persian squirrel (*Sciurus anomalus*) is a predominantly arboreal species, and accurate knowledge of its anatomy is important for clinical, conservation, and comparative purposes. The present study aimed to investigate the morphological and morphometric characteristics of the thoracic vertebrae, ribs, and sternum in this species using computed tomography (CT) and radiography.

Methods: In this study, the bony structures of the thoracic cavity were evaluated and measured. Quantitative data, including dimensions of thoracic vertebrae (T_1 to T_{12}), ribs, sternal segments, and thoracic indices, were extracted. Data analysis and parameter comparisons were performed using SPSS software and repeated-measures ANOVA at a significance level of $p < 0.05$.

Results: The results showed that the thoracic spine of the Persian squirrel has 12 vertebrae, with vertebral body length gradually increasing from T_1 to T_{12}. The tenth thoracic vertebra (T_{10}) was identified as the anticlinal vertebra. The thoracic cavity consisted of 12 pairs of ribs (8 true, 2 false, and 2 floating). The thoracic index (62.24%) and sternal morphology indicated a relatively wider laterolateral thoracic configuration, which may provide attachment areas for the pectoral musculature.

Conclusion: The osteological characteristics of the thoracic cavity in the Persian squirrel are consistent with a relatively conserved pattern within the Sciuridae family and are compatible with the locomotor demands associated with an arboreal lifestyle. These findings provide baseline anatomical information that may support future diagnostic and clinical studies in veterinary medicine**.**

Introduction

The thoracic cavity (Thorax) is one of the most important anatomical regions in the mammalian body, enclosed dorsally by the thoracic vertebrae, laterally by the ribs, and ventrally by the sternum (Orwoll, 1940). This structure not only provides a protective chamber for vital organs such as the heart, lungs, and great vessels but also functions as an expandable cylinder, facilitating the volumetric changes necessary for respiration and stabilizing the forelimbs during locomotion (Samuels & Van Valkenburgh, 2008; Schüler et al., 2024). A precise understanding of the anatomy and biomechanics of the thorax is essential not only for evaluating an animal's ability to withstand mechanical loads but also forms the foundation for clinical diagnostics (Soroori et al., 2022).

Among rodents, particularly within the family Sciuridae, the morphological characteristics of the vertebral column and thoracic cavity are directly correlated with locomotor type, lifestyle (arboreal, terrestrial, or gliding), and range of motion (Samuels & Van Valkenburgh, 2008; Kawashima et al., 2018). Comparative anatomical studies have demonstrated that the number of thoracic vertebrae and the position of the anticlinal vertebra follow a conservative yet flexible pattern within this family; the presence of 12 thoracic vertebrae and the anticlinal vertebra located at T_{10} (or T_9 in some species) are considered characteristic features of arboreal and gliding squirrels (Orwoll, 1940; Thorington, 1972; Thorington & Santana, 2007; Thippan et al., 2019). Furthermore, paleontological evaluations of early

fossil sciurids (e.g., Protosciurus) indicate structural stability of 12 thoracic vertebrae and skeletal features similar to extant species from the Oligocene to the present (Emry & Thorington, 1982; Linden et al., 2023).

The Persian squirrel (*Sciurus anomalus*) is the only representative of the family Sciuridae in the Middle East and southwestern Asia, a species that has been named after Iran (Akbari et al., 2024), playing a key ecological role (keystone species) in the regeneration and preservation of Zagros oak forests and adjacent regions (Thorington et al., 2012; Akbari et al., 2024). Based on taxonomic classifications, this species comprises three geographic subspecies: *S. a. anomalus*, *S. a. pallescens*, and *S. a. syriacus* (Thorington et al., 2012). Morphologically, the Persian squirrel is medium-sized (body weight ranging from 250 to 410 g) and, although primarily arboreal, limb studies have shown that its bones are shorter and more robust compared to the European red squirrel (Sciurus vulgaris), indicating a different degree of arboreality in this species (Thorington et al., 2012).

Despite its ecological importance, wide distribution, and increasing presentation as a pet to veterinary clinics, detailed and comprehensive osteological data on the thoracic region of this species remain unavailable (Sadeghinezhad et al., 2012; Akbari et al., 2024). Akbari et al. (2024), in their study on the adrenal gland of the Persian squirrel, emphasized the scarcity of anatomical data on this species and highlighted the importance of basic anatomical studies for diagnostic and therapeutic purposes. Today, advanced non-invasive diagnostic imaging methods such as computed tomography (CT) and digital radiography have become powerful tools for three-dimensional, precise, and non-destructive evaluation of bony structures in comparative anatomy of small mammals (Ruf, 2014; Soroori et al., 2022; Blake, 2024; Schüler et al., 2024).

Given the existing knowledge gap regarding the skeletal characteristics of the Persian squirrel and the urgent need for baseline data for clinical, conservation, and comparative anatomical purposes, the present study was designed and conducted to comprehensively investigate the morphology and morphometry of the thoracic vertebrae, ribs, and sternum in the Persian squirrel (*Sciurus anomalus*) using CT scanning and radiographic techniques.

Materials and Methods

2.1. Animals and Ethical Considerations

In the present study, five healthy adult male Persian squirrels (*Sciurus anomalus*) were examined at the Small Animal Hospital, Faculty of Veterinary Medicine, University of Tehran. The animals were referred to the hospital by the relevant environmental protection authority for the evaluation and management of non-vertebral clinical conditions. Radiographic and computed tomographic (CT) examinations were performed as part of their clinical assessment and were not conducted exclusively for research purposes. The imaging data obtained during these clinically indicated procedures were subsequently used for anatomical and morphometric analyses. Following completion of the clinical evaluations, the animals were returned to the relevant environmental protection authority.

Before imaging, the animals were housed individually in standard cages for seven days and maintained on a diet consisting of apples, carrots, and nuts (walnuts and acorns), with free access to water. For imaging procedures, the squirrels were transferred to the Small Animal Hospital and subjected to general anesthesia. Anesthesia was induced via intramuscular administration of ketamine (10%; 75 mg/kg) in combination with diazepam (1 mg/kg). The animals were monitored throughout the anesthetic and imaging procedures to minimize stress and discomfort.

The research project was reviewed by the Secretariat of the Biomedical Ethics Committee of the University of Tabriz. According to an official letter issued by the Vice-Chancellor's Office for Research and Technology of the University of Tabriz (Letter No. S-1017, dated 7 October 2026), the project was confirmed to comply with the applicable principles, regulations, and procedures of research ethics in biomedicine. This official letter was submitted to the journal as supporting documentation. No separate institutional ethics approval number was issued specifically for this study.

Radiographic Evaluation

Radiographic images were acquired using a digital radiography system (DirectView CR 850, Kodak) in the Radiology Department of the Faculty of Veterinary Medicine, University of Tehran. Dorsoventral (DV) and lateral radiographs of the vertebral column were obtained for each specimen. Exposure parameters were set at 45 kV and 4 mAs. All images were subsequently analyzed at the radiology workstation, where anatomical landmarks and vertebral features were identified and labeled.

Computed Tomography (CT) Scanning and Morphometric Analysis

Following radiography, the anesthetized animals were immediately transferred to the CT suite. Specimens were positioned in sternal recumbency on the couch of a multi-slice CT scanner (SOMATOM Spirit, Siemens). Transverse axial CT slices perpendicular to the long axis of the vertebral column were acquired with a slice thickness of 1.0 mm, a gantry rotation time of 1.0 s, a reconstruction interval ranging from 0.5 to 1.0 mm, a tube voltage of 120 kV, and a tube current of 100 mA. Consecutive scan datasets were processed using reconstruction algorithms to generate three-dimensional (3D) volume-rendered models and structural cross-sections of the vertebral column, ribs, and sternum.

Digital morphometric measurements—including **Vertebral Body Length (VBL), Vertebral Body Width (VBW), Vertebral Body Height (VBH), Vertebral Canal Width (VCW), Vertebral Canal Height (VCH), Spinous Process Length (SPL), Transverse Process Length (TPL), and Pedicle Height (PH)** for thoracic vertebrae; **Craniocaudal Length (CCL)** and **Lateromedial Width (LMW)** for ribs; and **Length, Thickness, and Height** for the sternum—were precisely performed on the sagittal, coronal, and 3D reconstructed CT slices using dedicated DICOM viewer software.

Statistical Analysis

Statistical analysis was performed using SPSS software (Version 26.0; IBM Corp., Armonk, NY, USA). The normality of quantitative data distribution (including measurements of thoracic vertebrae, ribs, sternum, and thoracic indices) was assessed using the Shapiro–Wilk test. All variables were expressed as mean ± standard deviation (Mean ± SD).

To evaluate differences in morphometric parameters across the thoracic vertebrae (T_1–T_{12}), ribs (R_1–R_{12}), and sternal segments, a repeated measures analysis of variance (Repeated Measures ANOVA) was conducted. When significant main effects were detected, the Bonferroni post-hoc test was applied for pairwise comparisons. For all statistical tests, a p-value of less than 0.05 ($p < 0.05$) was considered statistically significant.

Results

Anatomical & Morphological Findings

Thoracic Vertebrae

In the Persian squirrel (*Sciurus anomalus*), 12 thoracic vertebrae (T_1 to T_{12}) were observed. From cranial to caudal, the length of the vertebral bodies gradually increased and the bodies became more cylindrical. No ventral crest was present on any vertebra, and the ventral surface of all vertebrae was smooth. The spinous processes of T_1 to T_8 were long and directed caudally. The interspinous distances between T_1 and T_6 were wide; however, from T_6 onward, the spinous processes became closer to each other. The spinous process of T_{10} was oriented vertically, indicating the position of the anticlinal vertebra. The spinous processes of T_{11} and T_{12} were cranially inclined. Mammillary and accessory processes were observed from T_9 to T_{12}, which are associated with increased joint stability in the caudal thoracic region (Figs. 1–3).

Table 1
Morphometric parameters of thoracic vertebrae in the Persian squirrel (*Sciurus anomalus*) (Mean ± SD, mm)

vertebra	VCW	VCH	PH	SPL	TPL	VBH	VBW	VBL
T1	4.97 ± 0.41^{a}	2.83 ± 0.21^{ab}	1.61 ± 0.21^{c}	3.16 ± 0.40^{cd}	2.57 ± 0.31^{a}	2.13 ± 0.26^{bc}	5.51 ± 0.53^{a}	3.90 ± 0.50^{c}
T2	4.03 ± 0.48^{b}	2.85 ± 0.26^{ab}	1.47 ± 0.24^{c}	5.90 ± 1.03^{a}	2.53 ± 0.30^{a}	2.12 ± 0.33^{bc}	5.84 ± 0.61^{a}	3.61 ± 0.41^{c}
T3	3.83 ± 0.39^{bc}	2.83 ± 0.32^{ab}	1.78 ± 0.25^{bc}	6.23 ± 0.89^{a}	2.29 ± 0.28^{ab}	2.29 ± 0.31^{abc}	5.25 ± 0.56^{ab}	3.99 ± 0.43^{c}
T4	3.17 ± 0.34^{cd}	2.94 ± 0.28^{ab}	2.12 ± 0.21^{ab}	5.65 ± 0.67^{ab}	2.29 ± 0.34^{ab}	2.06 ± 0.27^{bc}	4.29 ± 0.46^{bc}	4.29 ± 0.53^{bc}
T5	3.12 ± 0.31^{cd}	2.64 ± 0.26^{ab}	2.64 ± 0.29^{a}	5.41 ± 0.53^{abc}	2.24 ± 0.29^{ab}	2.58 ± 0.32^{ab}	4.11 ± 0.39^{cd}	4.48 ± 0.58^{bc}
T6	3.11 ± 0.27^{cd}	3.12 ± 0.43^{a}	2.32 ± 0.28^{ab}	5.00 ± 0.56^{abc}	1.06 ± 0.20^{d}	2.41 ± 0.34^{abc}	4.11 ± 0.41^{cd}	4.73 ± 0.51^{abc}
T7	3.41 ± 0.32^{bcd}	2.10 ± 0.13^{b}	1.96 ± 0.22^{abc}	4.06 ± 0.51^{bcd}	1.71 ± 0.21^{bcd}	2.88 ± 0.30^{ab}	3.01 ± 0.32^{e}	5.30 ± 0.63^{abc}
T8	3.65 ± 0.37^{bcd}	2.35 ± 0.17^{ab}	2.12 ± 0.21^{ab}	3.88 ± 0.48^{bcd}	1.83 ± 0.26^{abc}	2.41 ± 0.28^{abc}	3.06 ± 0.28^{e}	5.32 ± 0.57^{abc}
T9	3.59 ± 0.26^{bcd}	2.53 ± 0.19^{ab}	1.70 ± 0.19^{bc}	3.70 ± 0.41^{cd}	1.67 ± 0.32^{bcd}	2.12 ± 0.21^{bc}	3.01 ± 0.26^{e}	5.41 ± 0.63^{ab}
T10	2.35 ± 0.21^{e}	2.36 ± 0.21^{ab}	1.88 ± 0.16^{abc}	3.17 ± 0.39^{cd}	1.41 ± 0.24^{cd}	2.71 ± 0.38^{ab}	3.36 ± 0.36^{de}	5.90 ± 0.54^{ab}
T11	3.06 ± 0.30^{cd}	2.18 ± 0.14^{b}	2.35 ± 0.23^{ab}	3.12 ± 0.31^{cd}	1.12 ± 0.19^{d}	2.53 ± 0.27^{ab}	3.41 ± 0.27^{de}	6.34 ± 0.62^{ab}
T12	3.00 ± 0.31^{d}	1.77 ± 0.10^{b}	2.27 ± 0.30^{ab}	2.01 ± 0.28^{d}	1.30 ± 0.17^{cd}	3.01 ± 0.34^{a}	3.53 ± 0.34^{cde}	6.45 ± 0.^{56a}
p-value	< 0.001	< 0.001	< 0.001	< 0.001	< 0.001	< 0.001	< 0.001	< 0.001

Note: Different superscript letters in each column indicate significant differences between vertebrae based on Bonferroni post-hoc test ($p < 0.05$).

Ribs

The thoracic cavity consisted of 12 pairs of ribs, divided into three groups: **8 pairs of true ribs** (attached to the sternum), **2 pairs of false ribs**, and **2 pairs of floating ribs** (R11and R_{12}). All ribs were arched and

possessed a long costal cartilage. From cranial to caudal, the capitulum approached the tuberculum, and in the last two ribs (R_{11} and R_{12}), these two structures fused to form a single articular surface. The ribs were compressed lateromedially and elongated craniocaudally. The costal cartilages were calcified in all specimens and clearly identifiable on radiographs and CT scans. The genu costae was located at the osteochondral junction in the first three ribs and within the cartilaginous portion in the remaining nine ribs (Figs. 1–3). The morphometric measurements of the ribs, including their dimensions and variations among different rib pairs, are presented in Table 2.

Table 2
Dimensions of ribs in the Persian squirrel (*Sciurus anomalus*) (Mean ± SD, mm)

vertebral	Lateromedial width	Craniocaudal length
R1	0.96 ± 0.05^{bc}	2.65 ± 0.14c
R2	0.91 ± 0.04^{c}	2.73 ± 0.15^{c}
R3	0.96 ± 0.05^{bc}	3.03 ± 0.18^{b}
R4	1.04 ± 0.06^{b}	3.23 ± 0.20^{b}
R5	1.15 ± 0.07^{b}	3.13 ± 0.19^{b}
R6	1.30 ± 0.08^{a}	4.41 ± 0.26^{a}
R7	1.30 ± 0.07^{a}	4.34 ± 0.25^{a}
R8	1.36 ± 0.08^{a}	3.58 ± 0.21^{b}
R9	1.29 ± 0.07^{a}	3.56 ± 0.22^{b}
R10	1.17 ± 0.06^{b}	3.46 ± 0.19^{b}
R11	1.28 ± 0.07^{a}	3.24 ± 0.18^{b}
R12	2.03 ± 0.11^{d}	2.03 ± 0.12^{d}
p-value	< 0.001	< 0.001

Note: Different superscript letters in each column indicate significant differences between ribs based on Bonferroni post-hoc test ($p < 0.05$).

Sternum

The sternum was elongated and curved, with a concave dorsal surface and a convex ventral surface. It consisted of **seven** cylindrical sternebrae, including the manubrium (first segment), five sternebral bodies (S_1 to S_5), and the xiphoid process. The clavicle articulated with the apex of the manubrium; the first rib attached to the manubrial body; and the second rib articulated at the joint between the manubrium and S_1. The caudal end of the xiphoid was dorsoventrally compressed, and ribs 7 and 8 attached to it. The morphometric measurements of the sternum, including its length, width, and other recorded dimensions, are summarized in Table 3.

Table 3
Dimensions of the sternum in the Persian squirrel (*Sciurus anomalus*)
(Mean ± SD, mm)

Sternal Segment	Length (L)	Thickness (T)	Height (H)
(Manubrium)	[illegible] ± [illegible]^{a}	[illegible] ± [illegible]^{a}	[illegible] ± [illegible]^{b}
Sternebra 1	[illegible] ± [illegible]^{c}	[illegible] ± [illegible]^{cd}	[illegible] ± [illegible]^{cd}
Sternebra 2	[illegible] ± [illegible]^{b}	[illegible] ± [illegible]^{b}	[illegible] ± [illegible]^{d}
Sternebra 3	[illegible] ± [illegible]^{b}	[illegible] ± [illegible]^{d}	[illegible] ± [illegible]^{ab}
Sternebra 4	[illegible] ± [illegible]^{c}	[illegible] ± [illegible]^{b}	[illegible] ± [illegible]^{bc}
Sternebra 5	[illegible] ± [illegible]^{bc}	[illegible] ± [illegible]^{b}	[illegible] ± [illegible]^{d}
Xiphoid	[illegible] ± [illegible]^{a}	[illegible] ± [illegible]^{e}	[illegible] ± [illegible]^{e}
p-value	< [illegible]	< [illegible]	< [illegible]

Note: Different superscript letters in each column indicate significant differences between sternal segments based on Bonferroni post-hoc test ($p < 0.05$).
The overall dimensions of the thoracic cavity were as follows: total sternal length, 48.5 ± 4.65 mm; maximum thoracic height (from the dorsal surface of the sternum to the ventral surface of the vertebral bodies), 20.6 ± 4.21 mm; and maximum thoracic width (from the internal surface of the thoracic wall), 33.1 ± 6.22 mm (Figs. 1–3).

Morphometric & Statistical Results

Morphometric evaluation was performed on five adult male Persian squirrels. The Shapiro–Wilk test confirmed normal distribution of all data ($p > 0.05$). Repeated measures ANOVA revealed significant differences among vertebrae, ribs, and sternal segments for all parameters ($p < 0.001$).

Morphometry of Thoracic Vertebrae (T_1–T_{12})

Based on the Bonferroni post-hoc test:

Vertebral Body Length (VBL)

Increased significantly from T_2 (3.61 ± 0.41 mm) to T_{12} (6.45 ± 0.56 mm) ($p < 0.05$). The greatest length was recorded at T_{12} and the least at T_2.

Vertebral Body Width (VBW)

The greatest value was recorded at T_2 (5.84 ± 0.61 mm), then decreased in the mid-thoracic region (T_7–T_9), with the lowest values at T_7 and T_9 (3.01 ± 0.26 mm) ($p < 0.05$).

Spinous Process Length (SPL)

Increased from T_1, peaking at T_3 (6.23 ± 0.89 mm), then progressively decreased caudally, with the lowest value recorded at T_{12} (2.01 ± 0.28 mm) ($p < 0.05$).

Vertebral Canal Width (VCW)

The greatest value was recorded at T_1 (4.97 ± 0.41 mm) and the lowest at the anticlinal vertebra (T_{10}) (2.35 ± 0.21 mm) ($p < 0.05$).

Other parameters (VCH, PH, TPL, and VBH)

The pattern of variation for each is presented in Table 1.

Morphometry of Ribs (R_1–R_{12})

Based on the Bonferroni post-hoc test:

Craniocaudal Length

Increased from R_1 (2.65 ± 0.14 mm) to R_6, reaching its maximum at R_6 (4.41 ± 0.26 mm), then decreased, with the minimum recorded at R_{12} (2.03 ± 0.12 mm) ($p < 0.05$).

Lateromedial Width

Increased from R_2 (0.91 ± 0.04 mm) to R_8 (1.36 ± 0.08 mm), remained relatively stable from R_9 to R_{11}, and reached its maximum at R_{12} (2.03 ± 0.11 mm) ($p < 0.05$).

Morphometry of the Sternum

Based on the Bonferroni post-hoc test:

Length (L)

The greatest length was observed in the manubrium (13.00 ± 2.70 mm) and xiphoid (11.90 ± 2.30 mm), which were significantly longer than all sternebral bodies (S_1–S_5) ($p < 0.05$).

Thickness (T)

The greatest thickness was recorded in the manubrium (3.10 ± 0.45 mm). The xiphoid (1.47 ± 0.22 mm) was the narrowest sternal segment ($p < 0.05$).

Height (H)

The greatest height was observed in S_3 (2.53 ± 0.31 mm) and the manubrium (2.49 ± 0.35 mm). The xiphoid (1.71 ± 0.23 mm) exhibited the lowest height ($p < 0.05$).

Morphometric Indices of the Thoracic Cavity

To further evaluate the proportions of the thoracic cavity in the Persian squirrel, six morphometric indices were calculated based on overall thoracic dimensions (Table 4).

Table 4
Morphometric indices of the thoracic cavity in Persian squirrel (*Sciurus anomalus*)

Index	Formula	Value	Interpretation
Thoracic Index	(Height ÷ Width) × 100	62.24	Thorax wider than tall (compressed dorsoventrally)
Length-Width Ratio	Sternal length ÷ Thoracic width	1.46	Elongated thoracic cavity
Height-Width Ratio	Thoracic height ÷ Thoracic width	0.62	Thorax wider than tall
Sternal Elongation Index	Sternal length ÷ Thoracic height	2.35	Highly elongated sternum
Cross-Sectional Area	Width × Height	681.86 mm^2	For interspecific comparison
Approximate Thoracic Volume	Length × Width × Height	33,074 mm^3	For interspecific comparison

Discussion

The findings of the present study revealed that the thoracic cavity of the Persian squirrel (*Sciurus anomalus*) possesses 12 thoracic vertebrae. This number is in agreement with previous reports in other arboreal squirrels, such as the eastern gray squirrel (*Sciurus carolinensis*) (Thorington, 1972), the red squirrel (*Sciurus vulgaris*) (Atalar & Yılmaz, 2004; Aydın, 2010), the genus *Microsciurus*, as well as the flying squirrels of the genus *Glaucomys* (Thorington & Santana, 2007). Furthermore, paleontological investigations on *Protosciurus* (the oldest fossil squirrel from the Oligocene period) have also reported the presence of 12 thoracic vertebrae (Emry & Thorington, 1982). The consistency of thoracic vertebral number among several extant and fossil sciurids may indicate a relatively conserved pattern within the

family Sciuridae (Bryant, 1945; Kawashima et al., 2018). In contrast, the report by Orwoll (1940) of 13 thoracic vertebrae in some North American species may reflect individual, geographical, or interspecific variation within Sciuridae.

In the present study, the tenth thoracic vertebra (T_{10}) was identified as the anticlinal vertebra—a point along the vertebral column where the orientation of the spinous processes changes from caudally inclined to approximately vertical and subsequently to cranially inclined. The location of the anticlinal vertebra at T_{10} in the Persian squirrel is consistent with findings in the eastern gray squirrel (Thorington, 1972), the Indian giant flying squirrel (Thippan et al., 2019; Koli, 2022), and the New Zealand white rabbit (Soroori et al., 2022). However, some reports in certain arboreal squirrels have indicated the anticlinal vertebra at T_9 (Atalar & Yılmaz, 2004). The variation in the position of the anticlinal vertebra may be associated with differences in the regional morphology and mobility of the thoracic vertebral column; however, the specific biomechanical significance of this variation in *S. anomalus* requires further investigation.

Additionally, the topographic position of internal organs in the Persian squirrel may be related to the arrangement of the thoracic vertebrae. Akbari et al. (2024) reported that the right adrenal gland is located beneath the tenth thoracic vertebra (T_{10}), while the left adrenal gland lies beneath the eleventh thoracic vertebra (T_{11}). This finding highlights the potential importance of accurate identification of thoracic vertebral levels when interpreting anatomical and imaging findings in this species (Akbari et al., 2024).

The gradual increase in vertebral body length (VBL) from the cranial to caudal thoracic region observed in the Persian squirrel is consistent with general trends reported in rodents and other sciurids (Kawashima et al., 2018; Hofmann et al., 2021; Linden et al., 2023). The elongation of the posterior thoracic vertebrae, together with the presence and development of accessory and mammillary processes in the mid- to caudal thoracic region, may contribute to regional spinal stability and provide attachment sites for deep back musculature. These morphological characteristics may be relevant to the mechanical demands of locomotion; however, direct biomechanical relationships were not evaluated in the present study.

The sternum of the Persian squirrel consists of seven distinct segments, including the manubrium, five sternebral bodies (S_1–S_5), and the xiphoid process. This number is consistent with the report by Thorington (1972) in the eastern gray squirrel, indicating a similar sternal organization among these arboreal squirrels. The sternum of the Persian squirrel is elongated, and its sternal-vertebral index indicates the relative extent of the sternum within the ventral aspect of the thoracic cavity. The relative development of the manubrium and the elongation of the sternal body may provide attachment areas for the pectoral musculature and may be compatible with the locomotor demands of arboreal species (Orwoll, 1940; Thorington & Santana, 2007; Schüler et al., 2024). Nevertheless, the relationship between these sternal characteristics and specific locomotor functions was not directly assessed in the present study.

In the thoracic cavity, 12 pairs of ribs were identified, including 8 pairs of true ribs, 2 pairs of false ribs, and 2 pairs of floating ribs. This arrangement is consistent with the findings reported in the present study and provides a detailed description of the rib configuration in *S. anomalus*. The observed arrangement can also be compared with descriptions available for other sciurid species (Orwoll, 1940).

Morphometric indices of the thoracic cavity provide a quantitative description of its overall proportions and may facilitate comparisons among species with different locomotor ecologies (Samuels & Van Valkenburgh, 2008). The thoracic index calculated for the Persian squirrel (62.24), together with the measured thoracic dimensions, indicates a thoracic cavity that is relatively wider laterolaterally and comparatively less deep dorsoventrally. Complementary anatomical information on the thoracic cavity of *S. anomalus* has been provided by Khaleel et al. (2022), who investigated the morphometric, histological, and histochemical characteristics of the lungs and trachea in this species. This configuration may be compatible with the general body form and locomotor requirements of an arboreal squirrel; however, the present morphometric data alone cannot establish a direct functional effect on maneuverability.

In comparison, flying squirrels (gliding squirrels), due to the requirements associated with patagium-supported locomotion, have been reported to exhibit differences in vertebral and thoracic morphology, including relatively longer lumbar vertebrae and differences in thoracic configuration (Thorington & Santana, 2007; Linden et al., 2023). On the other hand, ground squirrels (fossorial/ground squirrels), in association with the mechanical demands of burrowing and weight bearing, may exhibit a deeper and more laterally compressed thoracic cavity (Samuels & Van Valkenburgh, 2008). Therefore, the thoracic morphometric characteristics observed in the Persian squirrel are compatible with its arboreal ecology, although functional adaptation should be interpreted cautiously because locomotor performance and biomechanical parameters were not directly evaluated in this study.

The present study has several limitations that should be considered when interpreting the findings. The morphometric analysis was based on five adult male Persian squirrels; therefore, the findings may not represent variation associated with sex, age, body size, or geographic population. In addition, the present study focused on morphological and morphometric characteristics of the thoracic skeleton using radiography and CT and did not directly evaluate biomechanical performance or locomotor behavior. Accordingly, the potential relationships between thoracic morphology and arboreal locomotion should be interpreted as anatomical inferences rather than direct evidence of functional adaptation. Further studies involving larger and more diverse samples, together with biomechanical and functional assessments, may help clarify these relationships.

Conclusion

The present study provides a comprehensive description of the morphological and morphometric characteristics of the thoracic cavity, including the thoracic vertebrae, ribs, and sternum, in the Persian squirrel (*Sciurus anomalus*) using CT and radiographic imaging techniques. The presence of 12 thoracic vertebrae and the anticlinal vertebra at T_{10} is consistent with a relatively conserved pattern of thoracic

vertebral organization within the family Sciuridae (Bryant, 1945; Kawashima et al., 2018). Furthermore, the combination of features such as the relative development of the manubrium, elongation of the sternum, and the geometric proportions of the thoracic cavity is compatible with the locomotor demands associated with an arboreal lifestyle, although direct functional adaptation was not evaluated in the present study. The quantitative morphometric data provided by this study contribute to the comparative anatomical knowledge of the thorax in rodents and may provide baseline anatomical information for future diagnostic and clinical studies in wildlife and veterinary medicine.

Declarations

Consent for Publication

Not Applicable.

Ethical Statement

No animals were euthanized or sacrificed specifically for the purposes of this study. Radiographic and computed tomography (CT) examinations were performed on live adult Persian squirrels (*Sciurus anomalus*) referred to the Small Animal Hospital, Faculty of Veterinary Medicine, University of Tehran, by the relevant environmental protection authority for clinical evaluation. The imaging procedures were part of their clinical assessment and were not performed exclusively for research purposes. All procedures were conducted in accordance with applicable principles and regulations governing research ethics in biomedicine. The research project was reviewed by the Secretariat of the Biomedical Ethics Committee of the University of Tabriz, as confirmed by an official letter issued by the University's Vice-Chancellor's Office for Research and Technology (Letter No. S-1017, dated 7 October 2026). This letter was submitted to the journal as supporting documentation.

Conflicts of Interest

The authors declare no conflicts of interest.

Funding:

No funding.

Author Contribution

Ghasem Akbari and Atabak Shokrollahi conceived and designed the study; Ghasem Akbari, Atabak Shokrollahi performed the sample collection; Ghasem Akbari and Atabak Shokrollahi conducted the laboratory examination; Ghasem Akbari wrote the manuscript; Ghasem Akbari managed the project; Atabak Shokrollahi and Ghasem Akbari corrected the manuscript. All authors reviewed the manuscript.

Acknowledgement

We would like to thank Dr. Hamid Akbari and Mr. Sadeghi for helping us with the specimen collection.

Data Availability

The data that support the findings of this study are available from the corresponding author upon reasonable request.

References

1. 1. Akbari G, Hamidian G, Yaghmori M, Babaei M (2024) Anatomical, histochemical and stereological investigation of adrenal gland in persian squirrel (*Sciurus anomalus*). Vet Res Biol Prod 37:50–58. https://doi.org/10.22092/vj.2024.364665.2117
2. 2. Atalar O, Yılmaz S (2004) Anatomy of skeleton axiale of squirrel. Indian Vet J 81:305–311
3. 3. Aydın A (2010) The spinal nerves that constitute the plexus lumbosacrales of the red squirrel (Sciurus vulgaris). Vet Med 55:182–185
4. 4. Blake TE (2024) Factors that influence small mammal long bone morphology: An analysis of the femora, tibiae, and humeri of the eastern gray squirrel (Sciurus carolinensis). Master's thesis, Marshall University
5. 5. Bryant MD (1945) Phylogeny of Nearctic Sciuridae. Am Midl Nat 33:257–390
6. 6. Emry RJ, Thorington RW Jr (1982) Descriptive and comparative osteology of the oldest fossil squirrel, Protosciurus (Rodentia: Sciuridae). Smithson Contrib Paleobiol 47:1–35
7. 7. Hofmann R, Lehmann T, Warren DL, Ruf I (2021) The squirrel is in the detail: Anatomy and morphometry of the tail in Sciuromorpha (Rodentia, Mammalia). J Morphol 282:1659–1682. https://doi.org/10.1002/jmor.21412
8. 8. Kawashima T, Thorington RW Jr, Bohaska PW, Sato F (2018) Variability and constraint of vertebral formulae and proportions in colugos, tree shrews, and rodents, with special reference to vertebral modification by aerodynamic adaptation. Folia Morphol 77:44–56. https://doi.org/10.5603/FM.a2017.0064
9. 9. Khaleel IM, Al-Samarrae AS, Ibrahim RM (2022) Detection of morphometrical, histological and histochemical characteristics of lung and trachea in adult local squirrel (*Sciurus anomalus*). Rev Bionatura 7:1–7

10. 10. Koli VK (2022) Petaurista philippensis (Rodentia: Sciuridae). Mamm Species 54:1–10. https://doi.org/10.1093/mspecies/seac004
11. 11. Linden TJ, Burtner AE, Rickman J, McFeely A, Santana SE, Law CJ (2023) Scaling patterns of body plans differ among squirrel ecotypes. PeerJ 11:e14800. https://doi.org/10.7717/peerj.14800
12. 12. Orwoll HS (1940) The osteology and myology of the fox squirrel (Sciurus niger rufiventer), the gray squirrel (Sciurus carolinensis leucotis), and the red squirrel (Tamiasciurus hudsonicus loquax). Doctoral dissertation, Michigan State College of Agriculture and Applied Science
13. 13. Ruf I (2014) Comparative anatomy and systematic implications of the turbinal skeleton in Lagomorpha (Mammalia). Anat Rec 297:2031–2046. https://doi.org/10.1002/ar.23010
14. 14. Sadeghinezhad J, Tootian Z, Akbari GH, Chiocchetti R (2012) The topography and gross anatomy of the abdominal gastrointestinal tract of the Persian squirrel (*Sciurus anomalus*). Int J Morphol 30:524–530. https://doi.org/10.4067/S0717-95022012000200027
15. 15. Samuels JX, Van Valkenburgh B (2008) Skeletal indicators of locomotor adaptations in living and extinct rodents. J Morphol 269:1387–1411. https://doi.org/10.1002/jmor.10662
16. 16. Schüler S, Sharp AC, Nyakatura JA (2024) Comparative finite element analysis of the first thoracic vertebra in artiodactyls. J Morphol 285:e21695. https://doi.org/10.1002/jmor.21695
17. 17. Soroori S, Zehtabvar O, Amiri BS, Rostami A, Vali Y (2022) Evaluation of thoracic vertebrae in healthy White New Zealand rabbit (Oryctolagus Cuniculus): Computed tomographic and morphometric study. Vet Med Sci 8:1950–1957. https://doi.org/10.1002/vms3.847
18. 18. Thippan M, Lakshmishree KT, Dhoolappa M, Manjunath SS, Jayaramu GM, Vinay S (2019) Gross morphology and morphometrical studies on the vertebral column of Indian giant flying squirrel (Petaurista philippensis). Int J Livest Res 9:138–153. https://doi.org/10.5455/ijlr.20180809101415
19. 19. Thorington RW Jr (1972) Proportions and allometry in the gray squirrel, Sciurus carolinensis. Nemouria 8:1–17
20. 20. Thorington RW Jr, Koprowski JL, Steele MA, Whatton JF (2012) Squirrels of the World. Johns Hopkins University Press, Baltimore
21. 21. Thorington RW Jr, Santana EM (2007) How to make a flying squirrel: Glaucomys anatomy in phylogenetic perspective. J Mammal 88:840–853. https://doi.org/10.1644/06-MAMM-S-325R2.1

Figures

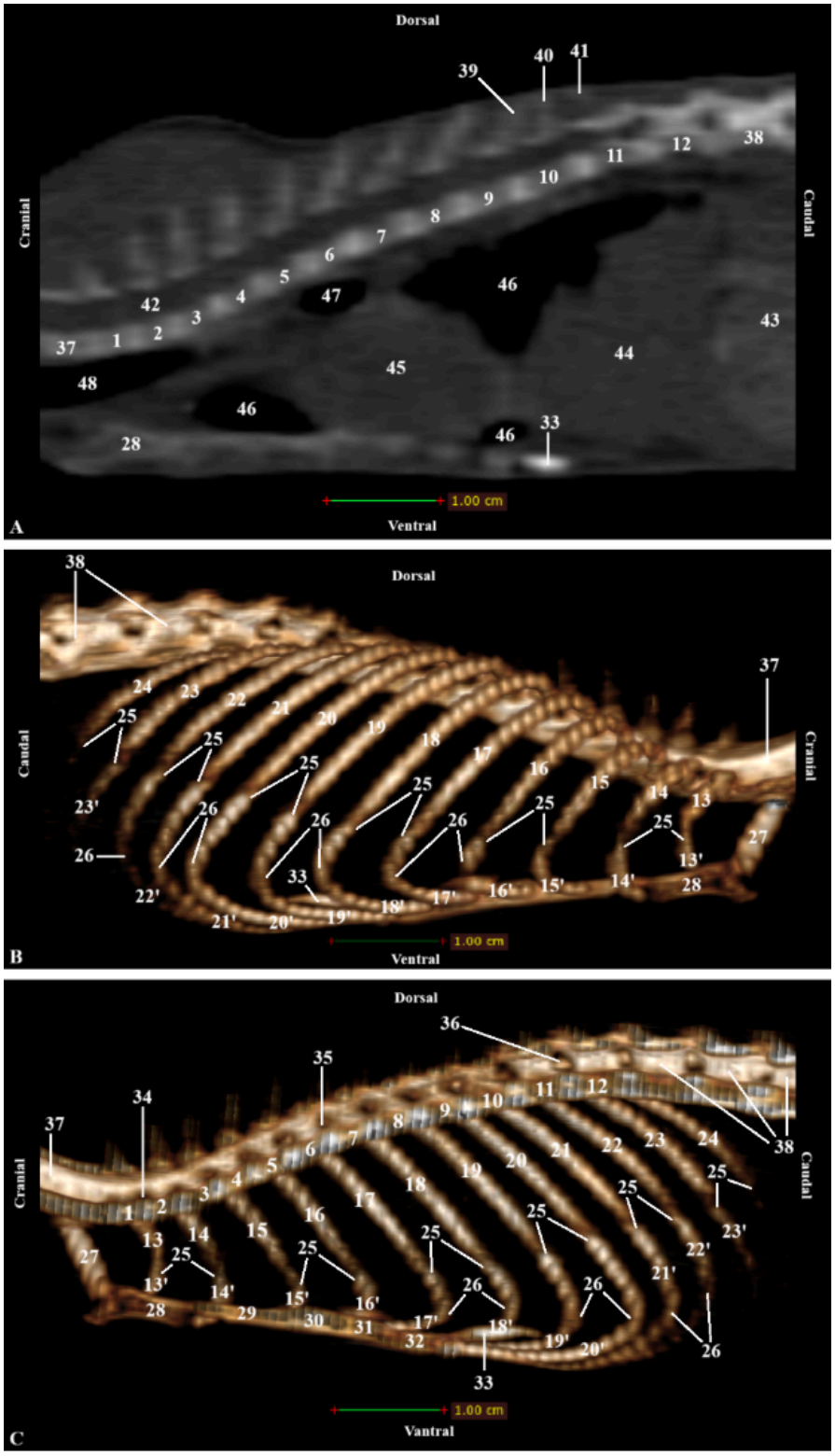

Figure 1

Midsagittal CT (A) and three-dimensional volume-rendered (B, C) images of the thoracic vertebrae and ribs of the Persian squirrel. 1–12, T1–T12 vertebral bodies; 13–24, bony parts of the 1st–12th ribs; 13'–23', corresponding 1st–11th costal cartilages; 25, costochondral junctions; 26, costal knees; 27, clavicle; 28, manubrium; 29–32, 1st–5th sternebrae; 33, xiphoid process; 34, T1–T2 intervertebral foramen; 35, T6–T7 intervertebral foramen; 36, T11–T12 intervertebral foramen; 37, cervical vertebrae; 38, lumbar

vertebrae; 39, spinous process of T9 (caudally directed); 40, spinous process of T10 (anticlinal vertebra); 41, spinous process of T11 (cranially directed); 42, vertebral canal; 43, stomach; 44, liver; 45, heart; 46, lung; 47, main bronchus; 48, trachea.

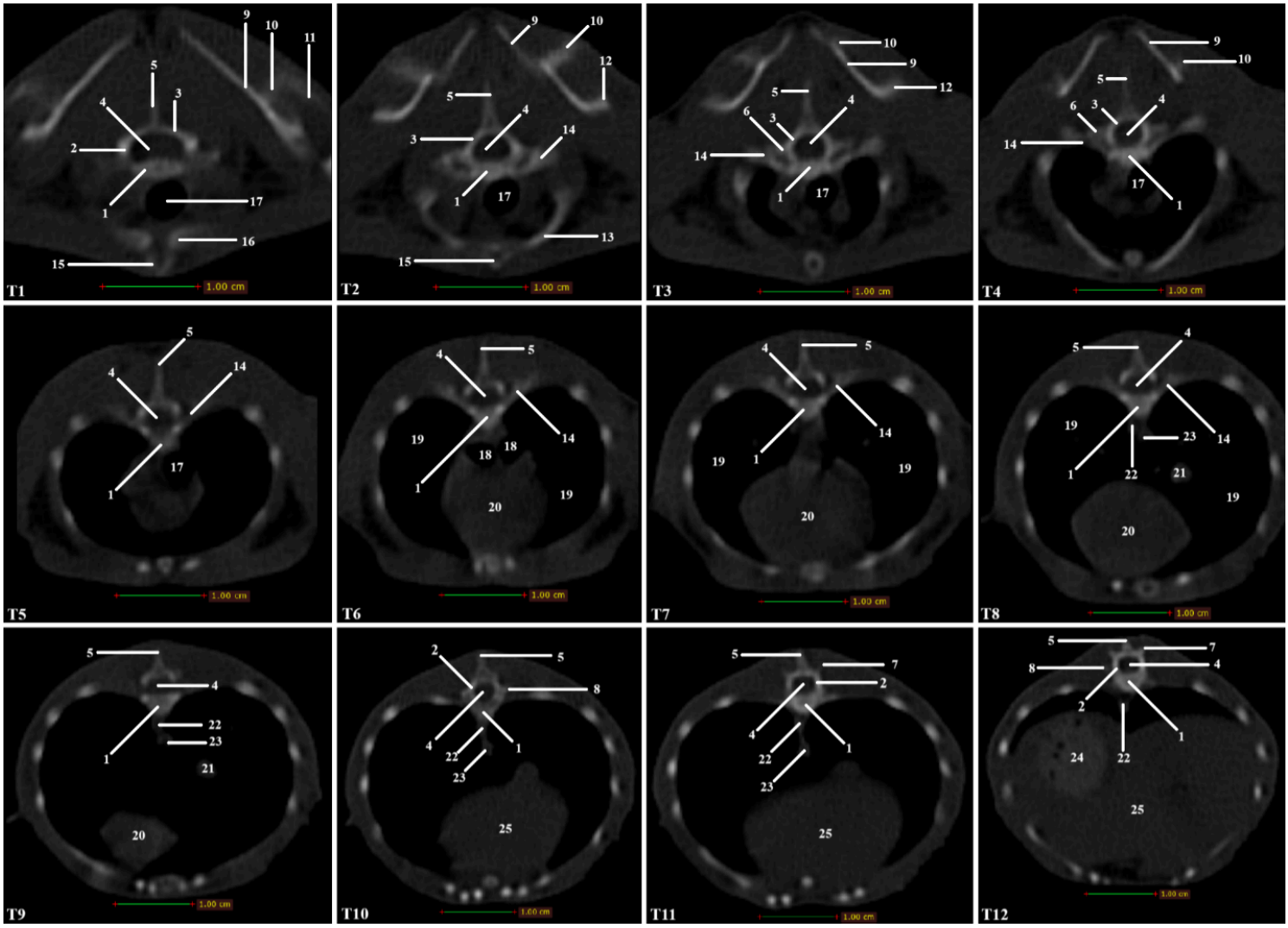

Figure 2

Transverse CT images through the T1–T12 thoracic vertebrae of the Persian squirrel. 1, vertebral bodies; 2, vertebral pedicles; 3, vertebral laminae; 4, vertebral foramina; 5, spinous processes; 6, transverse processes; 7, mammillary processes; 8, accessory processes; 9, scapula; 10, spine of the scapula; 11, metacromion process; 12, caudal spine of the spine of the scapula; 13, first rib; 14, ribs corresponding to each thoracic vertebra; 15, manubrium; 16, clavicle; 17, trachea; 18, mainstem bronchi; 19, lungs; 20, heart; 21, caudal vena cava; 22, aorta; 23, esophagus; 24, stomach; 25, liver. (WL: 428, WW: 1086).

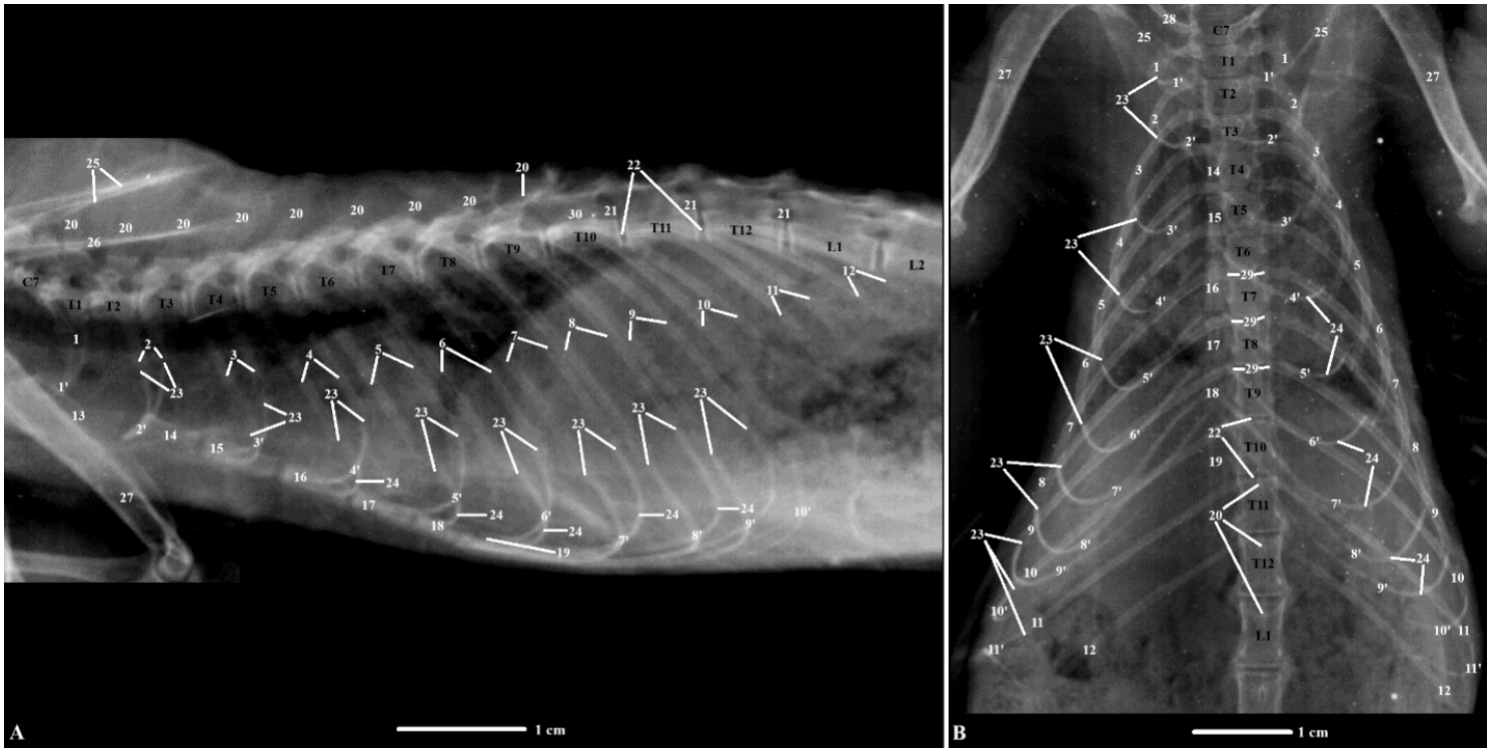

Figure 3

Lateral and ventrodorsal thoracic radiographs of the Persian squirrel. 1–12, osseous parts of the 1st–12th ribs; 1'–11', 1st–11th costal cartilages; 13, manubrium; 14–18, 1st–5th sternebrae; 19, xiphoid process; 20, spinous processes; 21, intervertebral foramina; 22, intervertebral disc spaces; 23, costochondral junctions; 24, costal knees; 25, spine of both scapulae; 26, caudal spine of the scapula; 27, humerus; 28, clavicle; 29, heads of the ribs; 30, vertebral canal.